DOI: 10.1002/ejic.200701305

"Hidden" Spin–Spin Interactions in Complex Multispin Solids

Elena V. Gorelik,*[a] Victor I. Ovcharenko,[a] and Martin Baumgarten[b]

Keywords: Density functional calculations / Magnetic properties / Heterospin exchange clusters / Nitronyl nitroxide radicals / Copper(II) complexes

A detailed analysis of the electronic structure and magnetic properties of a heterospin network based on a $Cu(hfac)_2$ complex with a nitronyl nitroxide biradical using the broken-symmetry density functional theory approach is reported. An extremely complex set of exchange parameters was revealed that cannot be obtained from the data of magnetochemical experiments alone. The compensating contributions from various exchange clusters show themselves in a sophisticated combination, and would be "hidden" without an in-depth quantum chemical investigation. For this purpose the extended network was subdivided into the dominating spin clusters bridged by the organic biradical spacer and each spin system was checked for a consistency of the spin couplings. Fairly large positive and negative exchange couplings in the strongly coupled clusters were found to cancel each other out. Furthermore, the detailed substructure analysis revealed that even in a linearly aligned spin system the next-nearest-neighbor interactions can be of the utmost importance and of similar size to that of the direct-neighbor exchange. Calculated exchange interaction parameters were employed to model the temperature dependence of the effective magnetic moment for the heterospin system under study. The use of PBE0 estimates of exchange interaction parameters yielded a $\mu_{eff}(T)$ dependence that was in good agreement with the experimental data, which enabled the data to be used as a starting point in the fitting procedure leading to the physical meaningful results.

Introduction

Progress in studies involving stable nitroxide chemistry has enabled the use of extended functionalized organic paramagnetic molecules in the design of molecular magnets. In reactions with metal ions, these radical-containing molecules provoke self-assembly towards rather complex structures.[1] The resulting solids are in general saturated with heterospin exchange clusters of various types. The energies of exchange interactions (J_i) in different clusters may be close in magnitude, which hinders their unambiguous assignment to the substructure of definite exchange clusters. Moreover, if the interactions, J_i, of a number of exchange clusters differ in sign, their mutual compensating contributions "smooth out" the functional features in the curve of the temperature dependence of χ or χT (or μ_{eff}). This makes it extremely difficult for researchers to derive exchange parameters from magnetochemical experiments. In fact, the accuracy of the exchange interaction parameters and their assignment to the particular exchange clusters from the data of magnetochemical experiments alone, in the case where more than two exchange channels turn out to be operative, are often ambiguous and questionable.

Recently, we encountered a striking example of this situation[2] when we described the magnetic properties of a heterospin solid formed by metal-biradical chains, whose structure is represented in Figure 1. The experimental curve $\mu_{eff}(T)$ for $[Cu(hfac)_2]_7(pyacbisNN)_2$ (**1**) has very few features. The value of μ_{eff} decreases from 6.15 to 5.68 μ_B as the temperature changes from 2 to 14 K, then it slightly increases (to 5.84 μ_B) when the temperature is increased further to about 50 K, and remains practically constant (from 5.84 to 5.88 μ_B) up to 300 K. The low-informative dependence $\mu_{eff}(T)$ does not allow us to suggest a justified scheme of exchange interactions in the chains and hence prompted us to perform a rigorous quantum chemical study.

This study unexpectedly revealed that the above-mentioned compensating contributions can present themselves in a sophisticated combination, and that they remain absolutely "hidden" in the absence of a quantum chemical investigation. In this paper we present a detailed analysis of the electronic structure and magnetic properties of the chain compound **1** using the broken-symmetry density functional theory (BS-DFT) approach. A physical meaningful fit of the temperature dependence of the magnetization curve was derived from this approach.

[a] International Tomography Center, Siberian Branch of the Russian Academy of Sciences,
Institutskaya 3a, 630090 Novosibirsk, Russia
Fax: +7-383-3331399
E-mail: lencha@tomo.nsc.ru
[b] Max Planck Institute for Polymer Research,
Ackermannweg 10, 55128 Mainz, Germany

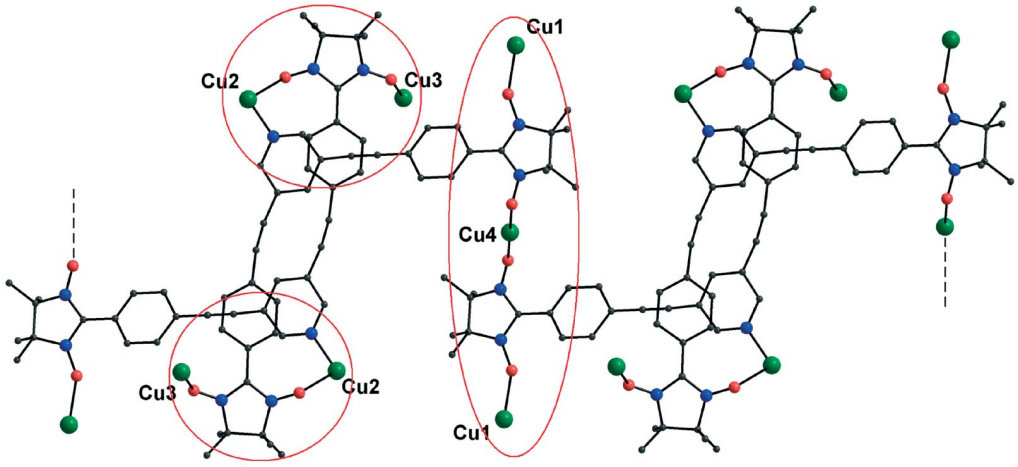

Figure 1. Ball-and-stick representation of chain **1**; H atoms and hfac fragments omitted for clarity. The red circles show the trimeric and pentameric spin motifs.

Results and Discussion

Choice of the Model

As shown in Figure 1, an X-ray structure analysis[2] indicated that each repeating unit in **1** carries a centrosymmetric cyclic six-spin cluster (within the two red circles) and a five-spin cluster (within the red ellipse). These repeating units include four different environments of the copper atoms possessing octahedral and trigonal-bipyramidal geometries (Figure 2). The structural data of the coordination units presented in Figure 2 undoubtedly show that exchange interactions within each cluster cannot be weak because of the close proximity of the metal and radical spins and can still have different signs for different coordination polyhedra.[3]

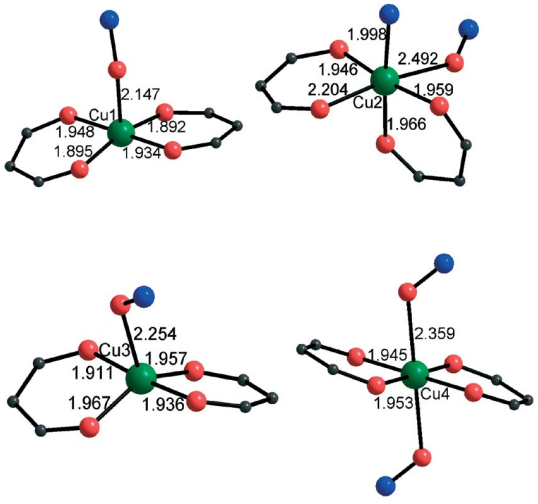

Figure 2. Different copper coordination sites inside the chain together with the coordination bond lengths in Å.

Thus the X-ray data of the structure of chain **1** show that each repeating unit of the chain carries three clusters of strongly coupled spins that are interconnected by phenylethynyl spacers. These are two equivalent three-spin clusters within the centrosymmetric six-spin cycle and the linear five-spin cluster, as is marked by the red lines in Figure 1. In order to figure out the dominating exchange pathways within **1** we followed the guidelines of the *bottom-up approach* that was suggested by Novoa et al.[4] We therefore started to examine, in depth, various spin subclusters within the coupled network and to check their consistency concerning signs and sizes of the exchange coupling parameters. In order to analyze the interplay of exchange interactions within **1** and elucidate the role of each of the pathways we considered a hierarchy of the model systems covering all the possible exchange pathways within the heterospin compound under study. Let us first examine in detail the clusters of strongly interacting spins, and then discuss the possible role of the exchange interaction channels through the phenylethynyl spacers.

It should be noted that the compounds containing both transition metal ions and nitronyl nitroxides represent a large class of heterospin clusters possessing interesting magnetic properties, at the same time they correspond to the most difficult case of quantum chemical calculations and analysis. The systems of interest are usually too big to be studied with elaborate post-Hartree–Fock methods, and the use of density functional theory (DFT) based approaches seems to be the only reasonable alternative. The latter approach nevertheless gives no universal recipe since the choice of the functionals to be applied is always up to the researcher and greatly depends upon the type of system considered. The use of hybrid functionals with a high percentage of exact Hartree–Fock exchange admixtures is generally recommended for the transition-metal-containing compounds,[5] and it was shown that the use of pure functionals may lead to a severe overestimation of the antiferromagnetic exchange interactions. At the same time hybrid functionals are not well suited to describe nitronyl nitroxide containing compounds because of the high spin contamination, which increases dramatically with the percentage of exact Hartree–Fock exchange.[6] Thus in order to get an insight into the magnetic properties of compound **1** we per-

formed calculations using both the gradient corrected PBE functional,[7] which was successfully applied to study exchange interactions in heterospin compounds,[8] and its hybrid version PBE0[9], which contains a 25% admixture of the exact Hartree–Fock exchange.

Another issue that should be addressed when using DFT methods is the treatment of open-shell states of the magnetic system. The most common choice is to use spin-polarized DFT calculations in combination with the broken-symmetry approach.[10] This has been demonstrated to be a powerful tool in the prediction and interpretation of magnetic properties of a large variety of magnetic systems, as well as for revealing and tracing magneto-structural correlations. At the same time the use of spin-adapted formalism always has an advantage when operating with electronic states, satisfying all the necessary symmetry requirements.[11] It was nevertheless shown that the common functionals lead to very poor results when used in spin-restricted DFT schemes such as the restricted ensemble Kohn–Sham formalism.[12] For this reason we will only consider the broken-symmetry (BS) approach.

The description of magnetic properties of compounds is usually based on the well-known phenomenological Heisenberg–Dirac–van Vleck (HDVV) spin Hamiltonian (1) describing isotropic exchange interactions between localized magnetic moments.

$$\hat{H}_{HDVV} = -2\Sigma J_{ij}\hat{S}_i\hat{S}_j \quad (1)$$

Since the broken-symmetry treatment results in solutions that are not the eigenstates of the $\hat{S}^2$ operator, the careful mapping of the broken-symmetry solutions onto the eigenstates of the spin Hamiltonian is required to extract the values of exchange interaction parameters from the results of the quantum chemical calculations.[13] One of the possibilities is to employ the original mapping procedure suggested by Noodleman et al.[14] or its more elaborated successor, the generalized spin projection (GSP) method developed by Yamaguchi et al.[15] Another way is to further simplify the spin Hamiltonian ending up at the well-known Ising model, see Equation (2), operating only with the z projection of the magnetic moments.

$$\hat{H}_{ISING} = -2\Sigma J_{ij}\hat{S}_i^z\hat{S}_j^z \quad (2)$$

This approach provides a straightforward way to obtain J values since the broken-symmetry solutions appear to be the eigenstates of the Ising spin Hamiltonian, at the same time being equivalent to the mapping procedure suggested by Noodleman.[13,16] While further discussing the computational results we will address both the Ising model and the generalized spin projection mapping procedure giving corresponding formulae to calculate exchange interaction parameters, although it appears that for the system under study both mapping approaches lead to very close values of exchange interaction parameters. This fact indicates that we are dealing with the case where the overlap of magnetic orbitals is small enough to be neglected during the exchange parameter estimation. Since the difference between Ising and Heisenberg exchange parameter values appears to be minor except for the case of the strong antiferromagnetic interactions,[15] in further discussions we will give only one set of parameters corresponding to the GSP method mentioning the difference in the results from these two mapping procedures where necessary.

The exchange interactions within the three- and five-spin clusters of the chain system **1** were traced using BS-DFT calculations on the model exchange clusters **2** and **3** shown in Figure 3. All the Cu···NN (NN means nitronyl nitroxide fragment) exchange interactions in spin systems **2** and **3** were expected to be rather strong due to the direct coordination of the nitroxide groups. In both model clusters the pyacbisNN biradical contribution between the copper centers was modeled by the NN-H radical shown in Scheme 1 and Figure 3.

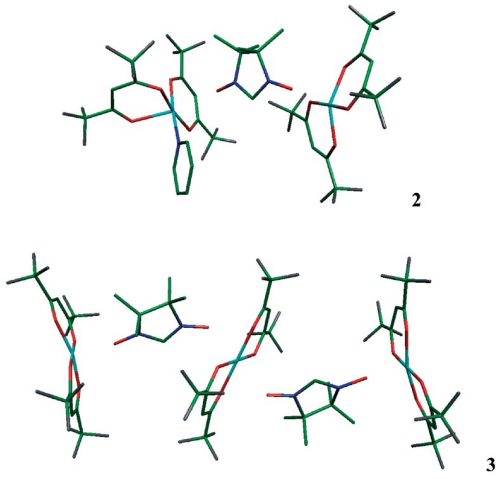

Figure 3. Structure of the model three-spin **2** and five-spin **3** clusters. H atoms are omitted for clarity.

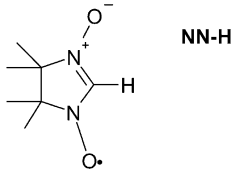

Scheme 1.

It was demonstrated previously[6a] that in the case of intermolecular exchange within pairs of NN radicals such a simplification of the ligand does not affect the direct exchange interactions. Hence, in the present case we could also expect only a negligible change in the picture of intracluster exchange interactions, although we are aware of a slightly enhanced spin density at the NO moieties compared to the phenyl-substituted nitronyl nitroxide NN-Ph because of some delocalization of spin into the phenyl ring.

It is a common practice to consider the exchange coupling with the nearest neighbors only, neglecting possible interactions with the next-nearest neighbors in linear systems. Nevertheless it was recently shown[17] that in some cases such interactions between next-nearest neighbors can play

a very important role. Bearing this in mind we will consider the schemes of exchange interactions in the model compounds **2** and **3** shown in Scheme 2.

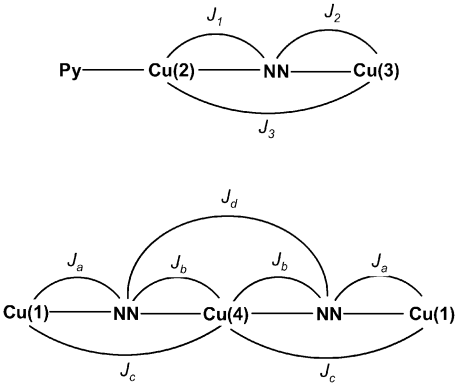

Scheme 2. The different exchange pathways in the subclusters **2** and **3** are considered.

On considering the structures of these three and five-spin motifs containing two and three Cu(hfac)$_2$ units, respectively, it was thought that the ligation of several metal units to the same NN fragment might perturb the spin density distribution in the radical, which in turn may significantly perturb corresponding exchange interactions. Sensitivity of the exchange interactions to the presence of another paramagnetic metal center coordinated to the same nitronyl nitroxide unit was tested using separate smaller parts of the model clusters **2** and **3**.

Three-Spin Cluster 2

Since most of the exchange clusters that we are going to consider contain several paramagnetic centers of different natures, we will first briefly summarize the models used to interpret the magnetic couplings in these clusters. Then we will outline the mapping of the corresponding spin Hamiltonians onto the total energy values of different spin configurations, which we obtain from quantum chemical calculations.

For the three-spin cluster Py–Cu(2)···NN···Cu(3) the HDVV spin Hamiltonian (1) takes the form shown in Equation (3).

$$\hat{H}_{HDVV} = -2J_1\hat{S}_{Cu(2)}\hat{S}_{NN} - 2J_2\hat{S}_{NN}\hat{S}_{Cu(3)} - 2J_3\hat{S}_{Cu(2)}\hat{S}_{Cu(3)} \quad (3)$$

In order to access all three exchange interaction parameters one has to construct four broken-symmetry solutions corresponding to different spin distributions over the cluster. The results of such calculations are summarized in Table 1.

Table 1. Spin configurations, total energies (in atomic units), and $<S^2>$ values for the set of broken-symmetry solutions used in the evaluation of exchange coupling parameters of **2**.

Spin configuration		PBE Total energy, E_i	$<S^2>_i$	PBE0 Total energy, E_i	$<S^2>_i$
1	ααα	–7820.622 4144	3.7623	–7820.745 8382	3.8126
2	αβα	–7820.623 3330	1.6437	–7820.745 7811	1.8052
3	ααβ	–7820.623 7274	1.6457	–7820.745 9466	1.8055
4	βαα	–7820.622 0057	1.7621	–7820.745 6730	1.8124

The exchange coupling parameters of the Hamiltonian (3) were calculated from the mean energies of the BS solutions listed in Table 1 by using the generalized spin projection (GSP) method[15] and the corresponding Ising spin Hamiltonian (see below).

$$J_1^{HDVV} = -\frac{E_1 - E_2 + E_3 - E_4}{<S^2>_1 - <S^2>_2 + <S^2>_3 - <S^2>_4}$$

$$J_2^{HDVV} = -\frac{E_1 - E_2 - E_3 + E_4}{<S^2>_1 - <S^2>_2 - <S^2>_3 + <S^2>_4}$$

$$J_3^{HDVV} = -\frac{E_1 + E_2 - E_3 - E_4}{<S^2>_1 + <S^2>_2 - <S^2>_3 - <S^2>_4}$$

$$J_1^{ISING} = -\frac{1}{2}(E_1 - E_2 + E_3 - E_4)$$

$$J_2^{ISING} = -\frac{1}{2}(E_1 - E_2 - E_3 + E_4)$$

$$J_3^{ISING} = -\frac{1}{2}(E_1 + E_2 - E_3 - E_4)$$

The motif Py–Cu(2)···NN···Cu(3) under consideration carries three paramagnetic centers each with spin 1/2. As can be seen from the data in Table 1, the presence of nitronyl nitroxide in the cluster leads to a significant increase of spin contamination with the inclusion of the exact Hartree–Fock exchange. Both PBE and PBE0 calculations give the same character of the exchange interaction channels although the magnitudes of all the interactions always appear to be much larger with PBE (as can be seen below, especially for the antiferromagnetic interactions J_2).

The calculations show that the interaction between spins localized on Cu(2) and NN is a rather strong ferromagnetic interaction as is usually supposed for axially coordinated NN radicals, with J_1(PBE) = +88 cm^{-1} as predicted by PBE, and J_1(PBE0) = +36 cm^{-1}. Nevertheless the same axial coordination of NN to Cu(3) leads to strong antiferromagnetic coupling. In this particular case the results from two mapping procedures are different giving J_2^{HDVV}(PBE) = –259 cm^{-1}, J_2^{ISING}(PBE) = –280 cm^{-1} for PBE calculations, while J_2^{HDVV}(PBE0) = J_2^{ISING}(PBE0) = –24 cm^{-1} for PBE0 calculations.

The exchange interaction J_3 between the next-nearest neighbors, namely between odd electrons localized on Cu(2) and Cu(3), is negligible in comparison to the other two couplings and does not affect the magnetic behavior of **2**: J_3(PBE) = +1.6 cm^{-1}, $|J_3(\text{PBE0})| < 0.1$ cm^{-1}. Consequently, this three-spin system possesses a low-spin ground state, which favors parallel spin orientation for Cu(2) and NN,

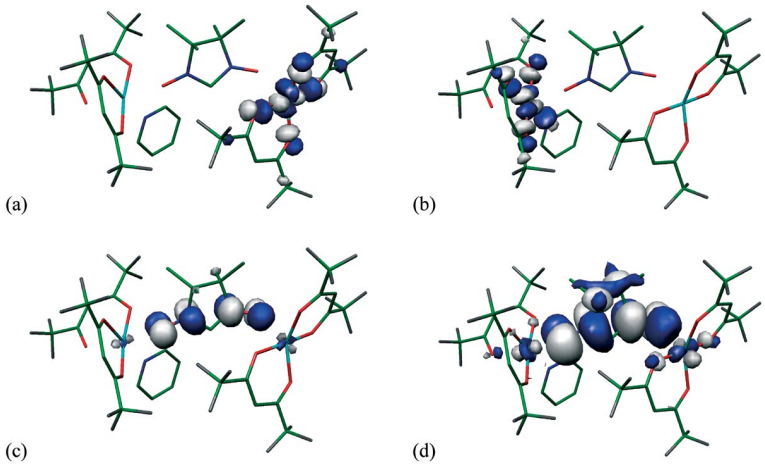

Figure 4. (a)–(c): Magnetic orbitals of the three-spin model cluster **2** from the high-spin PBE calculations. Orbital plots were made with a cutoff value of ϕ = ±0.05 a.u. (d) NN-centered magnetic orbital plotted with a cutoff value of ϕ = ±0.01 a.u. H atoms are omitted for clarity.

and antiparallel spin orientation for NN and Cu(3). This quite unusual picture of exchange interactions can be rationalized considering the magnetic orbitals of the trimeric motif. A view of the magnetic orbitals of **2** according to the data of PBE calculations for the ααα state corresponding to the maximum spin projection is presented in Figure 4.

Orbitals shown in Figure 4 (a and b) correspond to the singly occupied orbitals of the Cu(2) and Cu(3) centers, while the orbital in Figure 4 (c) is a NN-centered one. The latter has contributions from both Cu(2)- and Cu(3)-containing fragments. The character of such an admixture is very important for both the sign and the amplitude of the corresponding exchange interactions. As can clearly be seen from Figure 4 (d) this NN-centered magnetic orbital is orthogonal to the Cu(2)-centered one giving rise to the ferromagnetic exchange interaction between these two paramagnetic centers. At the same time the contribution from the Cu(3)-containing fragment into the NN-centered magnetic orbital appears to be nonorthogonal to the Cu(3)-centered magnetic orbital shown in Figure 4 (a), which manifests itself as a strong antiferromagnetic coupling of corresponding spins.

The analysis presented above shows that although the coupling to the next-nearest neighbor is negligible in this system, from the orbital picture presented in Figure 4, one may still expect some effect of the third magnetic center to be present. To check it we performed similar calculations on the isolated Py–Cu(2)···NN and NN···Cu(3) fragments representing two exchange channels of trimeric spin motif **2**. The comparison of the values obtained for these separate smaller parts of the model cluster **2** with those from the full three-spin system calculations shows that the presence of a third magnetic center in **2** changes the efficiency of the Cu···NN exchange channels, although it has no critical effect on the character of the interactions.

J_1(PBE) = +56 cm^{-1}

J_2^{ISING}(PBE) = –370 cm^{-1}; J_2^{HDVV}(PBE) = –328 cm^{-1}

J_1(PBE0) = +27 cm^{-1}; J_2(PBE0) = –32 cm^{-1}

It can be pointed out here that both functionals give similar trends in exchange interaction parameters when going from bigger clusters to the smaller subunits predicting the same character of exchange interactions. The comparison of the absolute values derived with different functionals shows that the known difference mainly concerns the amplitude or dramatic overestimation of antiferromagnetic interactions with PBE, as found here for J_2 and already explained in the previous section.

Linear Five-Spin Cluster 3

A similar analysis could be performed for the linear five-spin motif **3**. In this case, taking the centrosymmetric geometry of the cluster into account, the HDVV spin Hamiltonian takes the form shown in Equation (4).

$$\hat{H}_{HDVV} = -2J_a(\hat{S}_{Cu(1)}\hat{S}_{NN} + \hat{S}_{NN'}\hat{S}_{Cu'(1)}) - 2J_b(\hat{S}_{NN}\hat{S}_{Cu(4)} + \hat{S}_{Cu(4)}\hat{S}_{NN'}) - 2J_c(\hat{S}_{Cu(1)}\hat{S}_{Cu(4)} + \hat{S}_{Cu(4)}\hat{S}_{Cu'(1)}) - 2J_d\hat{S}_{NN}\hat{S}_{NN'} \quad (4)$$

The data on the set of spin configurations chosen to extract exchange interaction parameters for this system are summarized in Table 2.

Table 2. Spin configurations, total energies (in atomic units), and $<S^2>$ values for the set of broken-symmetry solutions used in the evaluation of exchange coupling parameters of **3**.

Spin configuration		PBE Total energy, E_i	$<S^2>_i$	PBE0 Total energy, E_i	$<S^2>_i$
1	ααααα	–11 625.744 4176	8.7729	–11 625.913 3735	8.8690
2	ααβαα	–11 625.743 4095	4.7720	–11 625.912 8121	4.8680
3	αβαβα	–11 625.743 0473	2.7713	–11 625.912 6250	2.8679
4	αααββ	–11 625.744 2848	2.7419	–11 625.913 1249	2.8673
5	ααααβ	–11 625.744 2391	4.7726	–11 625.913 2806	4.8690

The exchange-coupling parameters for **3** from the GSP approach are obtained as shown.

$$J_a^{HDVV} = -\frac{2E_1 + E_2 - E_3 - 2E_5}{2<S^2>_1 + <S^2>_2 - <S^2>_3 - 2<S^2>_5 - 6}$$

$$J_b^{HDVV} = -\frac{E_2 + E_3 - 2E_5}{<S^2>_2 + <S^2>_3 - 2<S^2>_5 - 2}$$

$$J_c^{HDVV} = -\frac{2E_1 - E_2 + E_3 - 2E_5}{2<S^2>_1 - <S^2>_2 + <S^2>_3 - 2<S^2>_5 - 2}$$

$$J_d^{HDVV} = -\frac{E_1 + E_2 - 2E_4}{<S^2>_1 + <S^2>_2 - 2<S^2>_4 - 6}$$

Mapping onto the Ising spin Hamiltonian gives

$$J_a^{ISING} = -\frac{1}{4}(2E_1 + E_2 - E_3 - 2E_5)$$

$$J_b^{ISING} = -\frac{1}{4}(-E_2 - E_3 + 2E_5)$$

$$J_c^{ISING} = -\frac{1}{4}(2E_1 - E_2 + E_3 - 2E_5)$$

$$J_d^{ISING} = -\frac{1}{2}(E_1 + E_2 - 2E_4)$$

Here similar trends for spin contamination and the amplitudes of exchange interactions are observed, and both PBE and PBE0 calculations confirm the ferromagnetic character of exchange interactions between neighboring spins suggested elsewhere:[2] J_a(PBE) = +40 cm^{-1} and J_b(PBE) = +111 cm^{-1}; J_a(PBE0) = +20 cm^{-1} and J_b(PBE0) = +62 cm^{-1}. Moreover, it can be seen that the superexchange channel between Cu(1) and Cu(4) is negligible, J_c(PBE) = –0.3 cm^{-1}, $|J_c(\text{PBE0})| < 0.1$ cm^{-1}; therefore Cu(1) is only coupled to the adjacent spin of NN.

The opposite situation takes place in the central three-spin cluster NN···Cu(4)···NN of the linear pentameric spin unit **3**, where the exchange coupling between the next-nearest neighbors appears to be significant, having antiferromagnetic character: J_d^{HDVV}(PBE) = –79 cm^{-1}, J_d^{ISING}(PBE) = –81 cm^{-1}; J_d^{HDVV}(PBE0) = J_d^{ISING}(PBE0) = –7 cm^{-1}. Thus the current system represents the case where an implicit consideration of the exchange interactions with the next-nearest neighbors is of crucial importance for the proper interpretation of magnetic properties. Orbital structural analysis reveals that the spins of NN radicals interact with each other by an efficient superexchange mechanism, mediated by a back-bonding interaction to the central metal (see Figure 5).

As a result of this interaction, despite the ferromagnetic character of exchange interaction between neighboring spin sites, the central NN···Cu(4)···NN three-spin cluster might have a low-spin ground state favoring an antiparallel orientation of NN spins. At this particular point PBE and PBE0 functionals predict opposite tendencies: while the gradient-corrected PBE functional predicts a low-spin ground state with a corresponding energy difference $E(S = 1/2) - E(S = 3/2) = 2J_d + J_b$ = –47 cm^{-1}, its hybrid analog PBE0 gives a high-spin ground state with $E(S = 1/2) - E(S = 3/2) = 2J_d + J_b$ = +48 cm^{-1}. This energy splitting is highly sensitive to the value of J_d and is the reason for the above mentioned difference in the ground state multiplicity predicted by PBE and PBE0 methods, although both methods give the same character of exchange interaction channels. In total this means that from the results of the DFT calculations we can not judge the multiplicity of the ground state of the linear five-spin cluster **5**, and its high- and low-spin states may be nearly degenerate.

The sensitivity of the values obtained from the presence of the second metal center ligated to the same NN fragment was checked using smaller isolated spin systems: Cu(1)··· NN and NN···Cu(4)···NN. These calculations yield J_a(PBE)

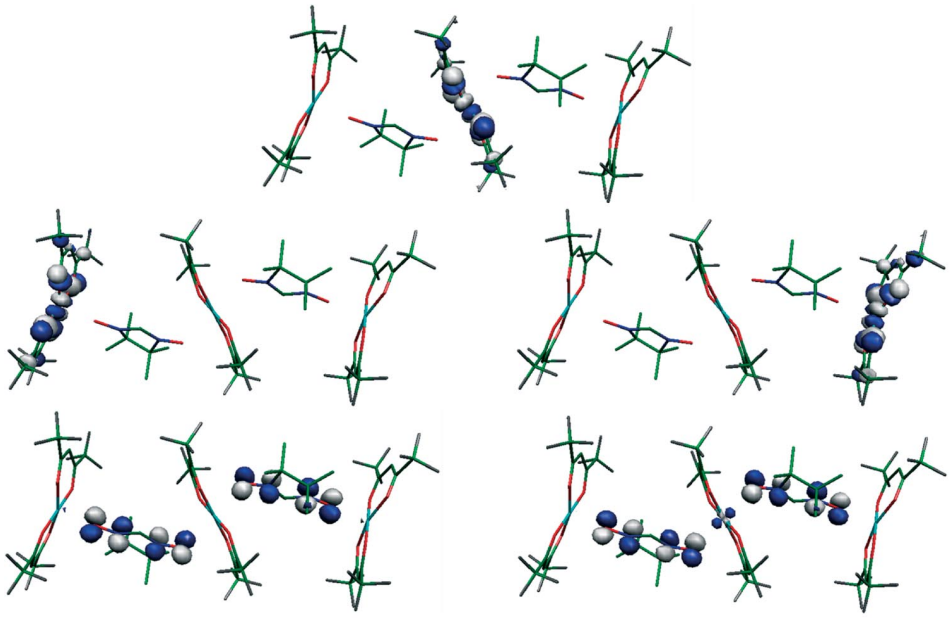

Figure 5. Magnetic orbitals of linear five-spin cluster model **3** from the high-spin PBE calculations. H atoms are omitted for clarity.

= +32 cm^{-1}, J_b(PBE) = +85 cm^{-1}, and J_d(PBE) = –54 cm^{-1} using the PBE functional, and J_a(PBE0) = +16 cm^{-1}, J_b(PBE0) = +47 cm^{-1}, and J_d(PBE0) = –5 cm^{-1} using PBE0. These results are in very good agreement with those obtained for the full five-spin linear cluster showing similar trends to the previously discussed calculations on the separate fragments of **2**.

Thus the calculations performed on model fragments **2** and **3** revealed the main exchange channels within **1** and allowed us to elucidate the electronic structure peculiarities that give rise to the unusual magnetic features in the system under study. Let us now turn to the discussion of much weaker exchange channels that nevertheless play an important role in the magnetic ordering within **1**.

Exchange Interactions Through the Phenylethynyl Spacers

Another important peculiarity of **1**, which has not been addressed so far, is the presence of the pyacbisNN biradical that acts not only as a chemical "bridging unit" but also as a magnetic one linking the clusters of strongly interacting spins into the sophisticated network. Exchange interactions through phenylethynyl spacers are much weaker in energy than the pathways within the trimeric and pentameric clusters considered above, but they are of crucial importance for the magnetic properties of the chain system **1** as they provide the coupling mechanism between the total spins of strongly interacting spin units.

The intramolecular exchange interaction in pyacbisNN biradical **4** is very important for the spin ordering in **1** since it governs the relative orientation of the total spins of trimeric **2** and pentameric **3** clusters. This is supposed to be a weak ferromagnetic interaction,[18] although no estimations based on DFT calculations have previously been done for **4**. The use of X-ray data on the structure of the pyacbisNN fragment within chain **1** gives J_{bir}(PBE) = +0.2 cm^{-1} and J_{bir}(PBE0) = +1.7 cm^{-1}, which is in good qualitative agreement with the data from the EPR spectroscopic experiments.[18]

The total spin of a cyclic six-spin cluster composed of two trimeric spin motifs **2** is governed by weak exchange interactions between Cu(2) and the pyacbisNN biradical coordinated by the pyridine nitrogen. Consideration of cluster **5** as shown in Figure 6 allows us to clarify the character of this interaction. In model cluster **5** we included only the Cu(2)···NN part of the trimeric spin system **2** that allows us to reduce the number of unpaired spins in the model cluster **5** providing nevertheless a reasonable estimate of operating exchange interactions.

Within the model four-spin-containing fragment **5** the exchange interaction pathways were considered as depicted in Scheme 3.

Because of the simplification mentioned above, the estimate of exchange parameter J_1 should be close to the value obtained for the Py–Cu(2)···NN isolated fragment. The HDVV spin Hamiltonian of the four-spin cluster **5** could be written as shown in Equation (5).

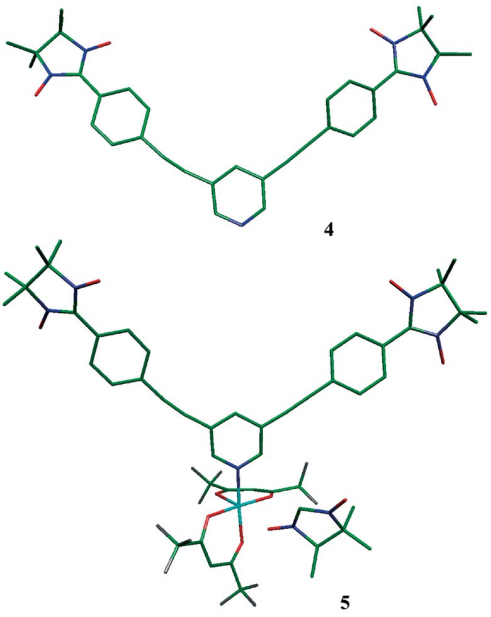

Figure 6. The structure of model clusters **4** and **5**. H atoms are omitted for clarity.

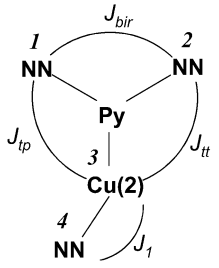

Scheme 3.

$$\hat{H}_{HDVV} = -2J_{bir}\hat{S}_1\hat{S}_2 - 2J_{tp}\hat{S}_1\hat{S}_3 - 2J_{tt}\hat{S}_2\hat{S}_3 - 2J_1\hat{S}_3\hat{S}_4 \quad (5)$$

where the numbering of the spin centers is shown in the scheme of exchange interactions. Here J_{tt} denotes the exchange interaction parameter from the phenylethynyl spacer connecting two three-spin units, while J_{tp} stands for the exchange interaction parameter from the spacer linking trimeric and pentameric spin units. The data on the set of spin configurations chosen to extract exchange interaction parameters for this system are given in Table 3.

Table 3. Spin configurations, total energies (in atomic units), and $<S^2>$ values for the set of broken-symmetry solutions used in the evaluation of exchange coupling parameters of **5**. The numbering of the spin centers is the same as that used in the scheme of exchange interactions.

Spin configuration		PBE Total energy, E_i	$<S^2>_i$	PBE0 Total energy, E_i	$<S^2>_i$
1	αααα	–5979.224 4419	6.0430	–5979.484 1628	6.2365
2	ααaβ	–5979.224 1983	3.0384	–5979.484 0410	3.2362
3	ααβα	–5979.224 1946	3.0382	–5979.484 0227	3.2348
4	αβαα	–5979.224 4397	3.0428	–5979.484 1460	3.2349
5	βααα	–5979.224 4394	3.0428	–5979.484 1467	3.2350

The following sets of equations were used to extract the exchange interaction parameters for **5** according to the GSP mapping procedure

$$J_1^{HDVV} = -\frac{E_1 - E_2}{<S^2>_1 - <S^2>_2 - 2}$$

$$J_{bir}^{HDVV} = -\frac{2E_1 - E_2 + E_3 - E_4 - E_5}{2<S^2>_1 - <S^2>_2 + <S^2>_3 - <S^2>_4 - <S^2>_5 - 4}$$

$$J_{tp}^{HDVV} = -\frac{E_2 - E_3 + E_4 - E_5}{<S^2>_2 - <S^2>_3 + <S^2>_4 - <S^2>_5 + 2}$$

$$J_{tt}^{HDVV} = -\frac{E_2 - E_3 - E_4 + E_5}{<S^2>_2 - <S^2>_3 - <S^2>_4 + <S^2>_5 + 2}$$

and according to the Ising model

$$J_1^{ISING} = -(E_1 - E_2)$$

$$J_{bir}^{ISING} = -\frac{1}{2}(2E_1 - E_2 + E_3 - E_4 - E_5)$$

$$J_{tp}^{ISING} = -\frac{1}{2}(E_2 - E_3 + E_4 - E_5)$$

$$J_{tt}^{ISING} = -\frac{1}{2}(E_2 - E_3 - E_4 + E_5)$$

As was expected, the values of J_1(PBE) = +54 cm^{-1} and J_1(PBE0) = +27 cm^{-1} derived from the calculations on **5** using the PBE and PBE0 functionals, respectively, are in excellent agreement with those obtained for the Py–Cu(2)···NN isolated cluster. The values of exchange interactions through phenylethynyl spacers are J_{tt}(PBE) = J_{tp}(PBE) = +0.4 cm^{-1}, J_{tt}(PBE0) = +2.1 cm^{-1}, J_{tp}(PBE0) = +1.9 cm^{-1}, and the estimate for the intramolecular interaction within the biradical is J_{bir}(PBE) = +0.1 cm^{-1}, J_{bir}(PBE0) = +1.6 cm^{-1}.

As mentioned above, the weak exchange interactions of Cu(2) and biradical **4** in the four-spin cluster **5** are responsible for the relative orientation of the total spins of the trimeric motifs in the cyclic six-spin cluster. On the other hand, intramolecular exchange interactions within biradical **4** are important for spin ordering in **1** since they govern the relative orientation of the total spins of adjacent trimeric **2** and pentameric **3** clusters. The data obtained demonstrate that spin ordering within the biradical and between the biradical and Cu(2) is ferromagnetic. However, these interaction pathways will only be effective at low temperatures.

Temperature Dependence of the Effective Magnetic Moment

The quantum chemical analysis discussed above provides us with an explicit magnetic structure of **1** together with estimates of corresponding exchange interaction parameters. The revealed sophisticated exchange interaction network inherent in the nature of **1** is summarized in Figure 7. Having this information on hand we can finally turn to the discussion of the temperature dependence of the effective magnetic moment.

The exact solution of such a complicated infinite spin arrangement is out of the scope of the present work, but the revealed hierarchy of the exchange interaction channels allows a simplified model to be employed. Since both PBE and PBE0 calculations demonstrate that all the exchange channels through phenylethynyl spacers are much less effective then those within the three-spin cluster **2** and linear five-spin cluster **3**, it appears reasonable to model the repeating unit of **1** by the combination of noninteracting five-spin and two three-spin fragments. The energy levels for spin multiplets E_n can be obtained by solving the corresponding spin Hamiltonian which is a linear combination of Equations (3) and (4). The temperature-dependent effective magnetic moment $\mu_{eff}(T)$ is evaluated as shown. The resulting calculated temperature dependencies using the exchange parameters from PBE and PBE0 calculations (summarized in Table 4), as well as the experimental $\mu_{eff}(T)$ curve are shown in Figure 8.

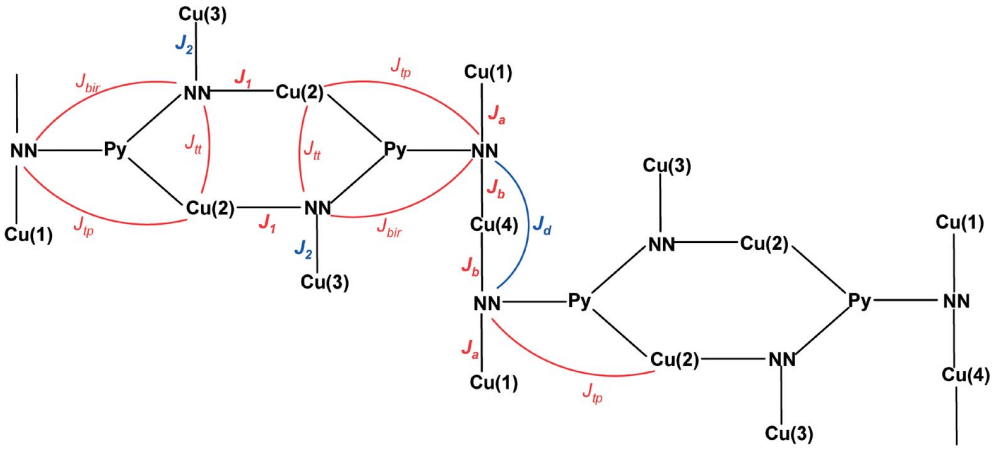

Figure 7. Scheme of exchange interactions in **1**. The channels shown in red are ferromagnetic, while the blue ones are antiferromagnetic.

Table 4. Estimates of exchange interaction parameters J [cm^{-1}] of the spin network **1** from PBE and PBE0 calculations. Parameters shown in bold were used in modeling the temperature dependence of the effective magnetic moment of **1**. The values obtained from experimental curve fitting are given in the last column for comparison.

	PBE	PBE0	Fit
$\boldsymbol{J_1}$	**+88**	**+36**	+8
$\boldsymbol{J_2}$	**–259**	**–24**	–17
J_3	1.6	<0.1	
$\boldsymbol{J_a}$	**+40**	**+20**	+9
$\boldsymbol{J_b}$	**+111**	**+62**	+15
J_c	–0.3	<0.1	
$\boldsymbol{J_d}$	**–79**	**–7**	–3
J_{bir}	+0.1	+1.6	
J_{tt}	+0.4	+2.1	
J_{tp}	+0.4	+1.9	

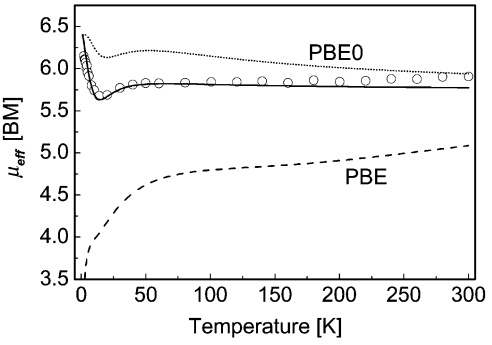

Figure 8. Calculated temperature dependence of the effective magnetic moment of the polymer compound **1** using exchange interaction parameters from PBE (dashed line) and PBE0 (dotted line) calculations as compared with the experimental $\mu_{eff}(T)$ curve[2] (o). Solid line shows the best fit with the parameters as described in the text.

$$\mu_{eff} = g\sqrt{\frac{\sum_n S_n(S_n+1)(2S_n+1)e^{-\beta E_n}}{\sum_n (2S_n+1)e^{-\beta E_n}}},\ \beta = 1/k_B T$$

The $\mu_{eff}(T)$ dependence calculated using PBE estimates of exchange interaction parameters appears to differ from the experimental curve, especially in the low-temperature region. The experimental temperature dependence shows a pronounced minimum at about 14 K with a subsequent increase in the magnetic moment when lowering the temperature down to 2 K. The calculated temperature dependence is on the contrary monotonic downward with temperature. The above mentioned low-spin ground state of the NN···Cu(4)···NN cluster predicted by PBE manifests itself at the low temperature limit of the calculated $\mu_{eff}(T)$ curve, while the slow increase of the calculated effective moment at high temperatures is predefined by the strong antiferromagnetic exchange channel J_2 in the three-spin cluster **2**.

The use of PBE0 estimates for the exchange interaction parameters, which are much more moderate then their PBE analogs, provides us with a curve that is in much better agreement with the experimental data; reproducing the low-temperature behavior together with a minimum at about 14 K. Overall the calculated high temperature dependence differs in character from that of the experimental curve, demonstrating some overestimation of the ferromagnetic components in the PBE0 calculation. At the same time variation of the exchange interaction parameters in reasonable limits enables a good reproduction of the experimental $\mu_{eff}(T)$ dependence for the whole temperature range. The resulting set of exchange interaction parameters is given in the last column of Table 4.

It should be emphasized that knowledge of the character and amplitude of the main exchange interaction channels is a prerequisite for such a modeling of the experimental data. Otherwise the abundance of interaction channels allows one to generate a horde of "best fitting" parameter sets and thus reproduce the observed $\mu_{eff}(T)$ dependence with no physical meaning. In the case of complicated heterospin compounds like the one discussed in this paper the quantum chemical calculations based on X-ray structural data serve as a unique approach that provides us with an insight into the magnetic structure of the compound.

Conclusions

The quantum chemical analysis that was performed allowed us to reconstruct the complicated picture of exchange pathways in **1**. A family of "hidden" interactions in the system of exchange parameters was revealed that could not be accessed from the data on magnetostatic experiments or from the qualitative analysis based on the X-ray structural data. It was shown that within the chain compound **1** it is possible to figure out a set of clusters of strongly interacting spins that are linked in a weak ferromagnetic manner by phenylethynyl spacers. The crucial role of the coupling between next-nearest neighbors in linear spin clusters on the total magnetic ordering was demonstrated.

With the calculated exchange interaction parameters a modeling of the experimental curve was performed, demonstrating that already for the PBE0 results quite a good similarity was obtained. Using these values as a starting point a fit was done enabling an even closer approximation of the $\mu_{eff}(T)$ but unlike for other curve fitting procedures a full understanding of the physical meaning is provided. The current approach thus opens the way to an in depth understanding of the magnetic properties of such inorganic–organic hybrid clusters.

Calculational Details

The calculations were performed using a DFT approach with the Gaussian-98 program.[19] In all the calculations the Wachters+f = (14s 11p 6d 3f)/[8s 6p 4d 1f] all-electron basis set was utilized for copper,[20,21] while the 6-31G(d) basis set was employed for all other atoms.[22] The exchange correlation was treated with the generalized gradient approximation after Perdew–Burke–Ernzerhof (PBE),[7] and using the parameter-free hybrid version PBE0 as suggested by Barone et al.[9] The generalized spin projection method was used

to determine the exchange interaction parameters as suggested by Yamaguchi et al.[15]

The geometries of fragments considered were taken from the X-ray diffraction determinations of chain **1**[2] without further optimization.

Acknowledgments

This research was supported by the Russian Foundation for Basic Research (grants 06-03-04000, 06-03-32742, 06-03-32157), the U.S. Civilian Research & Development Foundation (grant RUE1-2839-NO-06), and the President of Russia grant NSh-1213.2008.3. Further support through the Deutsche Forschungsgemeinschaft (DFG) grant 436 RUS 113/859/0-1 is also acknowledged.

[1] a) E. Tretyakov, S. Fokin, G. Romanenko, V. Ikorskii, S. Vasilevsky, V. Ovcharenko, *Inorg. Chem.* **2006**, *45*, 3671–3678; b) T. Ise, D. Shiomi, K. Sato, T. Takui, *Chem. Mater.* **2005**, *17*, 4486–4492; c) L. Catala, J. Le Moigne, N. Gruber, J. J. Novoa, P. Rabu, E. Belorizky, P. Turek, *Chem. Eur. J.* **2005**, *11*, 2440–2454; d) C. Stroh, E. Belorizky, P. Turek, H. Bolvin, R. Ziessel, *Inorg. Chem.* **2003**, *42*, 2938–2949; e) P. Taylor, P. R. Serwinski, P. M. Lahti, *Chem. Commun.* **2003**, 1400–1401; f) D. A. Shultz, K. E. Vostrikova, S. H. Bodnar, H.-J. Koo, M.-H. Whangbo, M. L. Kirk, E. C. Depperman, J. W. Kampf, *J. Am. Chem. Soc.* **2003**, *125*, 1607–1617; g) C. Stroh, R. Ziessel, *Chem. Commun.* **2002**, 1916–1917; h) Y. Hosokoshi, K. Katoh, Y. Nakazawa, H. Nakano, K. Inoue, *J. Am. Chem. Soc.* **2001**, *123*, 7921–7922; i) D. Shiomi, T. Kanaya, K. Sato, M. Mito, K. Takeda, T. Takui, *J. Am. Chem. Soc.* **2001**, *123*, 11823–11824; j) C. Rancurel, D. B. Leznoff, J.-P. Sutter, S. Golhen, L. Ouahab, J. Kliava, O. Kahn, *Inorg. Chem.* **1999**, *38*, 4753–4758; k) H. Oshio, M. Yamamoto, T. Ito, *J. Chem. Soc., Dalton Trans.* **1999**, 2641–2644; l) A. Caneschi, P. Chiesi, L. David, F. Ferraro, D. Gatteschi, R. Sessoli, *Inorg. Chem.* **1993**, *32*, 1445–1453.

[2] C. Rajadurai, V. Enkelmann, V. N. Ikorskii, V. I. Ovcharenko, M. Baumgarten, *Inorg. Chem.* **2006**, *45*, 9664–9669.

[3] a) F. L. de Panthou, D. Luneau, R. Musin, L. Öhrström, A. Grand, P. Turek, P. Rey, *Inorg. Chem.* **1996**, *35*, 3484–3491; b) V. I. Ovcharenko, G. V. Romanenko, V. N. Ikorskii, R. N. Musin, R. Z. Sagdeev, *Inorg. Chem.* **1994**, *33*, 3370–3381; c) R. N. Musin, P. V. Schastnev, S. A. Malinovskaya, *Inorg. Chem.* **1992**, *31*, 4118–4121.

[4] a) M. Deumal, M. J. Bearpark, J. J. Novoa, M. A. Robb, *J. Phys. Chem. A* **2002**, *106*, 1299–1315; b) L. Catala, J. Le Moigne, N. Gruber, J. J. Novoa, P. Rabu, E. Belorizky, P. Turek, *Chem. Eur. J.* **2005**, *11*, 2440–2454.

[5] a) R. L. Martin, F. Illas, *Phys. Rev. Lett.* **1997**, *79*, 1539–1542; b) F. Illas, R. L. Martin, *J. Chem. Phys.* **1998**, *108*, 2519–2527; c) Y. Takano, T. Soda, Y. Kitagawa, Y. Yoshioka, K. Yamaguchi, *Chem. Phys. Lett.* **1999**, *301*, 309–316.

[6] a) E. V. Gorelik, Yu. G. Shvedenkov, G. V. Romanenko, E. V. Tretyakov, V. I. Ovcharenko, 4th International Conference on Nitroxide Radicals: *Synthesis* Properties and Implications of Nitroxides, SPIN-2005, Novosibirsk, Russia, **2005**, p. 63; b) B. N. Plakhutin, E. V. Gorelik, N. N. Breslavskaya, M. A. Milov, A. A. Fokeyev, A. V. Novikov, T. E. Prokhorov, N. E. Polygalova, S. P. Dolin, L. I. Trakhtenberg, *J. Struct. Chem.* **2005**, *46*, 195–203.

[7] J. P. Perdew, K. Burke, M. Ernzerhof, *Phys. Rev. Lett.* **1996**, *77*, 3865–3868.

[8] a) A. V. Postnikov, A. V. Galakhov, S. Blugel, *Phase Transitions* **2005**, *78*, 689–699; b) E. V. Tretyakov, S. E. Tolstikov, E. V. Gorelik, M. V. Fedin, G. V. Romanenko, A. S. Bogomyakov, V. I. Ovcharenko, *Polyhedron* **2008**, *27*, 739–749.

[9] C. Adamo, M. Cossi, V. Barone, *J. Mol. Struct. (Theochem)* **1999**, *493*, 145–157.

[10] a) C. A. Daul, I. Ciofini, A. Bencini, in *Reviews of Modern Quantum Chemistry*, part II (Ed.: K. D. Sen), World Scientific, Singapore, **2002**, 1247–1294; b) L. Noodleman, C. Y. Peng, D. A. Case, J. M. Mouesca, *Coord. Chem. Rev.* **1995**, *144*, 199–244; c) L. Noodleman, J. G. Norman Jr, *J. Chem. Phys.* **1979**, *70*, 4903–4906.

[11] a) I. de P. R. Moreira, R. Costa, M. Filatov, F. Illas, *J. Chem. Theory Comput.* **2007**, *3*, 764–774; b) F. Illas, I. de P. R. Moreira, J. M. Bofill, M. Filatov, *Theor. Chem. Acc.* **2006**, *116*, 587–597.

[12] F. Illas, I. de P. R. Moreira, J. M. Bofill, M. Filatov, *Phys. Rev. B* **2004**, *70*, 132414 (4 pages).

[13] I. de P. R. Moreira, F. Illas, *Phys. Chem. Chem. Phys.* **2006**, *8*, 1645–1659.

[14] a) L. Noodleman, E. R. Davidson, *Chem. Phys.* **1986**, *109*, 131–143; b) L. Noodleman, *J. Chem. Phys.* **1981**, *74*, 5737–5743.

[15] a) M. Shoji, K. Koizumi, Y. Kitagawa, T. Kawakami, S. Yamanaka, M. Okumura, K. Yamaguchi, *Chem. Phys. Lett.* **2006**, *432*, 343–347; b) T. Soda, Y. Kitagawa, T. Onishi, Y. Takano, Y. Shigeta, H. Nagao, Y. Yoshioka, K. Yamaguchi, *Chem. Phys. Lett.* **2000**, *319*, 223–230; c) K. Yamaguchi, F. Jensen, A. Dorigo, K. N. Houk, *Chem. Phys. Lett.* **1988**, *149*, 537–542.

[16] D. Dai, M.-H. Whangbo, *J. Chem. Phys.* **2003**, *118*, 29–39.

[17] a) V. I. Ovcharenko, E. V. Gorelik, S. V. Fokin, G. V. Romanenko, V. N. Ikorskii, A. V. Krashilina, V. K. Cherkasov, G. A. Abakumov, *J. Am. Chem. Soc.* **2007**, *129*, 10512–10521; b) A. Rodriguez-Fortea, E. Ruiz, P. Alemany, S. Alvarez, *Monatsh. Chem.* **2003**, *134*, 307–316.

[18] C. Rajadurai, A. Ivanova, V. Enkelmann, M. Baumgarten, *J. Org. Chem.* **2003**, *68*, 9907–9915.

[19] M. J. Frisch, G. W. Trucks, H. B. Schlegel, G. E. Scuseria, M. A. Robb, J. R. Cheeseman, V. G. Zakrzewski, J. A. Montgomery, R. E. Stratmann Jr, J. C. Burant, S. Dapprich, J. M. Millam, A. D. Daniels, K. N. Kudin, M. C. Strain, O. Farkas, J. Tomasi, V. Barone, M. Cossi, R. Cammi, B. Mennucci, C. Pomelli, C. Adamo, S. Clifford, J. Ochterski, G. A. Petersson, P. Y. Ayala, Q. Cui, K. Morokuma, D. K. Malick, A. D. Rabuck, K. Raghavachari, J. B. Foresman, J. Cioslowski, J. V. Ortiz, A. G. Baboul, B. B. Stefanov, G. Liu, A. Liashenko, P. Piskorz, I. Komaromi, R. Gomperts, R. L. Martin, D. J. Fox, T. Keith, M. A. Al-Laham, C. Y. Peng, A. Nanayakkara, M. Challacombe, P. M. W. Gill, B. Johnson, W. Chen, M. W. Wong, J. L. Andres, C. Gonzalez, M. Head-Gordon, E. S. Replogle, J. A. Pople, *Gaussian 98*, Gaussian Inc., Pittsburgh PA, **1998**.

[20] a) A. J. H. Wachters, *J. Chem. Phys.* **1970**, *52*, 1033–1036; b) A. J. H. Wachters, *IBM Tech. Rept*. RJ584 (**1969**); c) C. W. Bauschlicher, S. R. Langhoff Jr, L. A. Barnes, *J. Chem. Phys.* **1989**, *91*, 2399–2411.

[21] Basis sets were obtained from the Extensible Computational Chemistry Environment Basis Set Database, Version 02/02/06, as developed and distributed by the Molecular Science Computing Facility, Environmental and Molecular Sciences Laboratory, which is part of the Pacific Northwest Laboratory, P. O. Box 999, Richland, Washington 99352, USA, and funded by the U. S. Department of Energy. The Pacific Northwest Laboratory is a multi-program laboratory operated by Battelle Memorial Institute for the U. S. Department of Energy under contract DE-AC06-76RLO 1830. Contact Karen Schuchardt for further information.

[22] E. R. Davidson, D. Feller, *Chem. Rev.* **1986**, *86*, 681–696.

Received: December 2, 2007
Published Online: May 15, 2008

